Supplementary Information For:

Stable Solar-Driven Water Oxidation to O_2(g) by Ni Oxide Coated Silicon Photoanodes

Ke Sun[1,2], Matthew T. McDowell[1,2], Adam C. Nielander[1], Shu Hu[1,2], Matthew R. Shaner[1,2], Fan Yang[1,2], Bruce S. Brunschwig[3], Nathan Lewis*[1-4]

[1] Division of Chemistry and Chemical Engineering, California Institute of Technology, Pasadena, CA 91125, USA.

[2] Joint Center for Artificial Photosynthesis, California Institute of Technology, Pasadena, CA 91125, USA.

[3] Beckman Institute and Molecular Materials Research Center, California Institute of Technology, Pasadena, CA 91125, USA.

[4] Kavli Nanoscience Institute, California Institute of Technology, Pasadena, CA 91125, USA.

*Correspondence to: nslewis@caltech.edu

Experimental Procedures

Materials and Chemicals

All materials were used as received, except where otherwise noted. The chemicals used were: sulfuric acid (H_2SO_4, J. T. Baker, ACS reagent, 95%-98%), concentrated hydrochloric acid (HCl, Sigma Aldrich, ACS Reagent 37%), hydrogen peroxide (H_2O_2, Macron Chemicals, ACS grade

30%), concentrated ammonium hydroxide (NH_4OH, Sigma Aldrich, ACS reagent 28%-30%), Buffered HF Improved (Transene Company Inc.), potassium hydroxide pellets (KOH, Macron Chemicals, ACS 88%), potassium ferrocyanide trihydrate ($K_4Fe(CN)_6 \cdot 3H_2O$, Acros, >99%), potassium ferricyanide ($K_3Fe(CN)_6$, Fisher Chemicals, certified ACS 99.4%), iron(II) sulfate heptahydrate ($FeSO_4 \cdot 7H_2O$, ReagentPlus eagentPluslusFeSO, certified AC_3, Sigma Aldrich, reagent grade 97%), zinc powder (Zn, Sigma Aldrich, dust <10μm, ≥98%), and potassium chloride (KCl, Macron Chemicals, Granular ACS 99.6%). Water with a resistivity of 18.2 MΩ·cm was obtained from a Millipore deionized water system.

Preparation of Substrates and Fabrication of Emitter

An np^+-Si sample coated by FTO glass, with the p^+ emitter layer fabricated using ion implantation, was obtained from the Joint Center for Artificial Photosynthesis at Lawrence Berkeley National Laboratory. The detailed fabrication of the emitter onto a single-side polished Czochralski-grown n-type (P-doped) prime-grade, (100)-oriented Si wafer has been described elsewhere.[1] The FTO glass was removed from these samples as described previously [2]. Briefly, the FTO-coated np^+-Si was immersed in a mixture of 0.5 M HCl, 0.4 M $FeSO_4$, and 0.1 M $FeCl_3$ and then the mixture was agitated while ~3.5 g Zn was slowly poured into the mixture. The solution turned clear after ~2 min and the samples were then removed and rinsed with deionized water. To remove any surface metal contaminants, the samples were immersed for ~30 s in an oxidizing solution that contained 1.0 M HCl and 0.5 M $FeCl_3$, and the samples were then removed from the solution and rinsed. Samples were then further cleaned using an RCA clean, as described below.

Three types of Si wafers, all with diameters of 3", were used: p^+-Si(111) and p^+-Si(100) (B-doped with a resistivity, $\rho < 0.002$ Ω·cm, 380±25 μm thick, prime grade, Addison Engineering, Inc.); and n-Si(111) (P-doped with $\rho = 0.1–1$ Ω·cm, UniversityWafer, Inc.). The wafers, and the np^+-Si samples from which the FTO coating had been removed, were cleaned using an RCA SC-1 procedure of soaking in a solution of NH_4OH:H_2O_2:H_2O (6:1:1, by volume) for 20 min at 70 °C. The wafers were then rinsed, dried, and placed in Buffer HF Improved for ~ 10 s. The samples were then rinsed and etched using the RCA SC-2 procedure of soaking in a solution of HCl:H_2O_2:H_2O (6:1:1, by volume) for 20 min at 70 °C. Samples were thoroughly rinsed with deionized water and were dried using N_2(g).

Deposition of NiO_x and Ni Metal Coatings

Reactive RF sputtering was performed using an AJA high-vacuum magnetron sputtering system (AJA International Inc.) with a chamber having a maximum base pressure of 8×10^{-8} Torr. The Ar/O_2 ratio was 20, while the Ar flow was held constant at 20 sccm and the working pressure was held at 5 mTorr. The substrates were held at 300 °C. The RF power on the Ni target (Kurt Lesker, 2" diameter × 0.125" thickness, 99.95%) was maintained at 150 W. The deposition rate was kept low, in the range of 0.42-0.62 Å/s, and therefore the deposition time was normally ~20-30 min, depending on the aging of the sputtering target. The same conditions were used to deposit metallic Ni, except that the stage was not heated and O_2(g) was not supplied. The deposition times under these conditions were normally ~ 2-3 min, depending on the aging of the sputtering target.

Preparation of Electrodes

Ohmic contacts to the back sides of Si samples were formed by scribing an In-Ga eutectic alloy (Alfa Aesar, 99.99%) onto the unpolished surfaces. High-purity Ag paint (SPI supplies) was then used to mechanically attach the ohmic contact to a coiled, tin-plated Cu wire (McMaster-Carr) which was then threaded through a glass tube (Corning Incorporation, Pyrex tubing, 7740 glass). The sample was then encapsulated and sealed to the glass tube using a mixture of 2:1 grey epoxy (Hysol 9460F) and white epoxy (Hysol 1C). The epoxy was typically allowed to set under ambient laboratory conditions for mechanically attach the ohmic contused. A high-resolution optical scanner (Epson Perfection V370 with a resolution of 2400 psi) was used to image the exposed surface area of each electrode, and the geometric areas were determined by analyzing the images using ImageJ software. All of the electrodes used in this study were ~ 0.1 cm^2 in area unless otherwise specified.

Electrochemical Measurements

A Mercury/Mercury oxide (Hg/HgO in 1.0 M KOH, CH Instruments, CH152) electrode was used as the reference electrode, and a carbon cloth placed within a fritted glass tube (gas dispersion tube Pro-D, Aceglass, Inc.) was used as the counter electrode for all electrochemical measurements performed in 1.0 M KOH(aq) electrolyte, including photoelectrochemical, spectral response, and faradaic efficiency measurements. The equilibrium potential for the oxygen evolution reaction (OER) was determined to be 0.32 V versus the Hg/HgO reference based on the measured pH of the solution (pH 14). A custom electrochemical cell with a flat glass (Pyrex) bottom was used for all of the electrochemical measurements. During measurements, the electrolyte was vigorously agitated with a magnetic stir bar driven by a model-train motor (Pittman) with a Railpower 1370 speed controller (Model Rectifier Corporation). The data

presented for electrochemical measurements in aqueous solutions do not include compensation for the series resistance of the solution. ELH-type (Sylvania/Osram) and ENH-type (EIKO) tungsten-halogen lamps with a custom housing and powered by a transformer (Staco Energy Products Co.) were used for long-term photoelectrochemical stability measurements. A Xenon arc lamp (Newport 67005 and 69911) equipped with an infrared filter (Newport 61945) and an AM 1.5G filter (Newport 81094 and 71260) was used as the light source for *J-E* and spectral response measurements. The illumination intensity at the position of the working electrode in the electrochemical cell was determined by placing a calibrated Si photodiode (FDS100-Cal, Thor Labs) into the cell at the same position occupied by the exposed area of a photoelectrode. To illuminate bottom-facing photoelectrodes, a quartz diffuser (Newport 15Diff-Vis) together with a broad-band reflection mirror (Newport dielectric mirror, 10Q20PR-HR) was used to bend the uniform light beam from the horizontal to the vertical direction.

Cyclic voltammetry as well as quantum efficiency measurements were performed using a Biologic SP-200 potentiostat (Bio-Logic Science Instruments). Cyclic voltammetric data were obtained at a constant scan rate of 40 mV s^{-1} and the scan range varied depending on the photovoltage of the sample. The quantum yield was measured using the potentiostat with the current output connected to a lock-in amplifier, and the incident light was chopped at a frequency of 20 Hz.

Electrochemical Impedance Spectroscopy and Mott-Schottky Analysis

Electrochemical impedance spectroscopy was used on n-Si|NiO_x, n^+-Si|NiO_x, and p^+-Si|NiO_x to determine the barrier height of the n-Si|NiO_x interface and the doping level of NiO_x. The measurement was conducted in solution of 50 mM $K_3Fe(CN)_6$, 350 mM $K_4Fe(CN)_6$, and 1.0 M

KCl in 200 mL of H_2O. The reverse bias dependence of the area-normalized semiconductor depletion-region capacitance is given by the Mott-Schottky relation:

$$\frac{1}{C^2} = \left(\frac{2}{A^2 q N_d \varepsilon_0 \varepsilon_r}\right)\left(\phi_b - V_n - \frac{k_b T}{q} - V_{app}\right)$$

where A is the device area, N_d is the donor impurity concentration in the semiconductor, $\square_0$ is the vacuum permittivity, and $\square_r$ is the relative permittivity, q is electron charge, $\square_b$ is the C-V barrier height, V_n is the voltage difference between the potential of the Fermi level and the potential off the conduction-band edge of the n-type semiconductor in the bulk, k_b is the Boltzmann constant, T is the temperature in K, and V_{app} is the difference between the applied potential and the redox potential of the solution. A Mott-Schottky (M-S) plot of C^{-2} versus V_{app} should be linear with a slope related to N_d and an x-intercept related to $\square_b$. M-S plots obtained from the impedance data for the devices were linear (R^2>0.9999).

The doping level was calculated based on the equation:

$$N_d = \frac{2}{A^2 q \varepsilon_0 \varepsilon_r \left[\frac{d(1/C^2)}{dV_{app}}\right]}$$

where $(d(1/C^2)/dV_{app})$ is the slope of the M-S plot. The solution was quiescent and was kept in the dark during the measurements. The electrochemical impedance data were fit to a model that consisted of a parallel resistor and a capacitor with a fixed constant-phase element at the Si|NiO_x interface arranged electrically in series with another resistor and capacitor in parallel at the NiO_x/electrolyte interface.

The dielectric constant of NiO_x was determined from the measured refractive index using the equation:

$$\varepsilon' = n^2 - k^2$$

where ε' is the real part of the complex dielectric constant and n is the refractive index and k is the extinction coefficient. The values of n and k were determined using spectroscopic ellipsometry (vide infra).

The average value of N_d extracted from the M-S slope (2×10^{16} cm^{-3}) of n-Si|NiO_x was in excellent agreement with the range specified by the manufacturer (5×10^{16}~5×10^{15} cm^{-3}), confirming that the measured capacitance was indeed the depletion-region capacitance at the Si|NiO_x interface. The M-S slope for p^+-Si|NiO_x was expected to be ~ 2.4×10^{13}– 2.4×10^{12} $F^{-2}m^4V^{-1}$, which was consistent with the measured slopes. The average value of N_d extracted for p^+-Si|NiO_x was ~ 10^{19} cm^{-3}.

Measurements of the Faradaic Efficiency of Oxygen Evolution

A Neofox fluorescence probe (Foxy probe, Ocean Optics) was used to monitor the concentration of oxygen throughout the experiment. The fluorescence response was calibrated against the standard concentration of oxygen in water (7700 μg L^{-1} or 2.4×10^{-4} M) under a standard 20.9% (by volume) oxygen atmosphere. The fluorescence probe, the Hg/HgO/1.0 M KOH reference electrode, a fritted Pt mesh counter electrode (Alfa-Aesar, 100 mesh, 99.9% trace metal basis), and the np^+-Si|NiO_x working electrode with a geometric surface area of 0.79 cm^2 were loaded into an air-tight glass cell that had a volume of 43.6 mL with no headspace, and that was equipped with four ports and a side-facing quartz window. The cell and the 1.0 M KOH electrolyte used in the cell were purged with a stream of ultra-high purity Ar(g) for ~2 h prior to the measurement.

The oxygen-concentration data were converted into micrograms of O_2 by first correcting for the O_2 leak rate measured during the first 10 min of the experiment, followed by calculating the mass of O_2 in micrograms at each time point. The calculation was performed by multiplying the reported percentage of oxygen by the number of micrograms of O_2 dissolved in water at room

temperature under 1 atm of pressure, 7700 μg L^{-1} (assuming the value is the same as for 1.0 M aqueous acidic solutions), and by the cell volume (43.6 mL), and dividing by the concentration of O_2 in air under 1 atm as reported by the florescence probe (20.9%). To compare the charge versus time data from the potentiostat with the amount of oxygen generated versus time for a system operating at 100% faradaic efficiency, the charge passed (in mA·h) was multiplied by 3.6 to convert the data into coulombs, and the result was then multiplied by 83 (the factor for conversion of 1 C of electrons to 1 μg of O_2) to convert the value into micrograms of O_2. Therefore, both the cumulative oxygen generated and charge passed during the measurement can be shown in one plot with two comparable y-axes, where 0.32 mA·h of charge passed corresponded to 100 μg O_2 generated.

Scanning-Electron Microscopy and Atomic-Force Microscopy

Scanning-electron microscopy (SEM) imaging was performed using a Nova NanoSEM 450 (FEI) with an accelerating voltage of 5 kV. Atomic-force microscopy (AFM) images were collected using a Bruker Dimension Icon microscope operating in ScanAsyst mode and using Bruker ScanAsyst-Air probes (silicon tip on a silicon nitride cantilever, spring constant: 0.4 N m^{-1}, frequency: 50-90 kHz, Al back coating) for p^+-Si|NiO_x with a thickness of 35~160 nm. The scan size was typically 1 μm × 1 μm. The images were analyzed using NanoScope software version 1.5. Flattening was performed to remove curvature and slope from images.

UV-Visible Absorption Measurements

The optical absorption of the NiO_x- or Ni metal-coated Si was determined by using an integrating sphere at normal incidence (Agilent Cary 5000 UV-Vis spectrometer). The absorption of NiO_x-coated Si was determined by subtracting the measured reflection and transmission from unity.

The optical transmission of NiO_x and ultrathin Ni metal on quartz substrates were also measured using the integrating sphere and were normalized against the transmission of bare quartz substrates. Tauc plot was generated by plotting $h\nu$ versus $(ah\nu)^2$, where α is the absorption coefficient determined based on the Beer-Lambert law. The band gap of the NiO_x at the onset of significant absorption, as well as interband absorption, were determined by a linear extrapolation of the optical absorption edge to the y axis of the Tauc plot.

Spectroscopic Ellipsometry

The complex refractive index (n, k) data for the NiO_x coatings were measured on p^+-Si substrates with a thickness of 35~160 nm and were determined using spectroscopic ellipsometry by fitting the data according to a general oscillator model that assumed that an intermediate 2 nm native oxide (SiO_2) formed during sputtering. Moreover, a rough surface with a thickness of 5 nm was considered based on the AFM measurements of roughness, to include the air/NiO_x mixture. The measurement was conducted using a J.A. Woolam V-VASE system. The n and k values were extracted from a normal fit, using a fixed film thickness based on the calibrated cross-sectional SEM measurement. The absorption coefficient can be also calculated using equation: $\alpha = 4\pi\kappa/\lambda$. κ is the extinction coefficient, which is the imaginary part of the complex refractive index obtained from fitting of the ellipsometric data. The position of the absorption peak in the visible region was consistent with the absorption features extracted from the Tauc plot using the UV-vis measurement.

X-ray diffraction spectroscopy

XRD analysis was conducted using Bruker D8 Discover system equipped with 2-dimentional Vantec-500 detector. Cu-Ka radiation (1.54 Å) was generated at a tube voltage of 1 kV and a tube

current of 50 mA. The incident beam was focused using a mono-capillary collimator. A laser beam marks the focal spot on the specimen fixed on a xyz stage. The scattered diffraction was registered by a 2-dementional detector with an angular resolution of the detector smaller than 0.04 degree, and enables the simultaneous detection of the diffraction data in a 2theta range of 20 degree. The detected radiation was counted for 2000 sec to obtain an appropriate XRD profile. Data were analyzed using Bruker EVA software.

Load-line analysis and definition of photovoltaic properties

The details of a load-line analysis can be found in references 3,4. Briefly, the photoelectrode performance is treated in a simplified equivalent circuit approach as a photovoltaic cell connected in series electrically with a dark electrolysis cell. The photovoltaic parameters including the open-circuit voltage (V_{oc}), the short-circuit current density (J_{sc}), the fill factor (FF) and the energy-conversion efficiency (η) are then evaluated by subtracting the dark electrolysis J-E data obtained using a p^+-Si|NiO_x dark electrode from the J-E data exhibited by the illuminated photoelectrode under evaluation.

Estimation of the lower limit of total Turnover number, percentage of active Ni atoms, charge required for dissolving the entire Si photoelectrode, and branching ratio of water oxidation relative to Si oxidation

To estimate the lower limit on the turnover frequency per active site, a lattice constant of 0.4195 nm was used for a cubic NiO crystal with a NaCl structure. The unit cell contained 4 Ni atoms and the density of the Ni atoms in the NiO was calculated using the number of atoms divided by the cell volume, which is 5.42×10^{22} cm^{-3}. The turnover frequency[5,6] in the unit of number of O_2

molecule per second per electrochemical active Ni atom can be calculated assuming a constant current density of 32 mA cm^{-2} (j) using equation

$$TOF = \frac{j \cdot 6.02 \times 10^{23}}{1000 \cdot 96485 \cdot 4} \cdot \frac{1}{N_{Ni} A t_{NiO}} = 0.18 \frac{O_2}{s} \; per \; Ni \; atom$$

Therefore, the total turnover number (TON) is TOF*4320000 s which is around 0.8×10^6.

The percentage of active Ni atoms in the film based on the reductive peak area in the Ni redox peak region was calculated as follows:

$$Ni\% = \frac{Q_{act} \cdot 6.24 \times 10^{18}}{N_{Ni} t_{NiO}}$$

where Q_{act} is the charge density (based on the peak area) in mC cm^{-2} associated with the quantity of electroactive Ni atoms on the surface.

The total charge passed during the 1200 h of chronoamperometry was ~144000 C cm^{-2}. The charge needed to dissolve the Si photoelectrode was calculated by first calculating the atom density following the same approach used for calculating the density of Ni atoms in NiO. The Si diamond lattice constant of 0.543 nm was used with 8 Si atoms in each unit cell. The Si atom density was ~5×10^{22} cm^{-3}. To break the Si–Si bond during etching in KOH involves 4 electrons. Therefore, the total charge needed can be calculated by multiplying the atom density, surface area, the Si wafer thickness of 400 μm, and the elementary charge of 1.6×10^{-19} coulombs:

$$Q_{Si} = 4NAt_{Si}q$$

To estimate the branching ratio of water oxidation relative to Si oxidation, it was assumed that 10 nm of uniform SiO_2 would fully passivate the Si surface. This was conservative because if thinner SiO_2 (3-4 nm) were fully passivating, then the branching ratio estimate would increase by a factor of 2-3. The total charge needed to form 10 nm of SiO_2 was then calculated by multiplying

the Si atom density, thickness of the oxide, expansion coefficient assuming that the volume expansion occurred in one direction normal to the surface (1/2.2), and the elementary charge.

$$Q_{ox} = 4NAt_{ox}q/2.2$$

The branching ratio was then given by Q_{ox}/Q_{total}.

Supplementary Figures

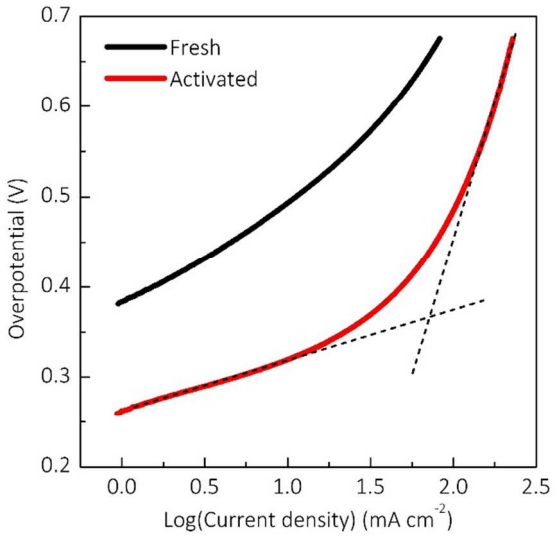

Figure S1. Tafel plots for the oxygen-evolution reaction at p^+-Si|NiO_x electrodes in 1.0 M KOH(aq) before (black line) and after (red) ten cyclic voltammetric scans.

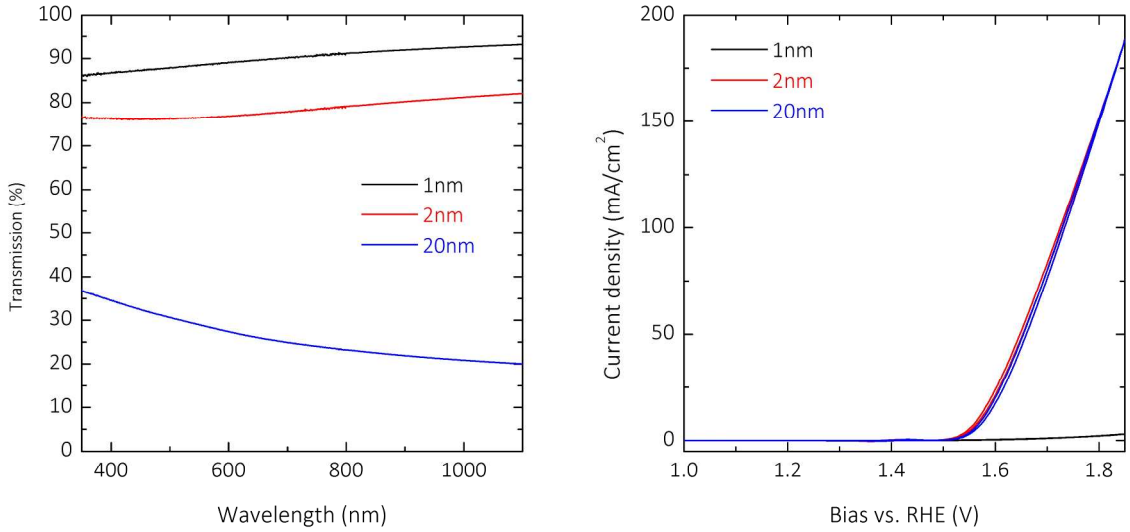

Figure S2. Transmission of metallic Ni coated quartz substrates and catalytic activity measured on metallic Ni coated p^+-Si substrates in 1.0 M KOH(aq)

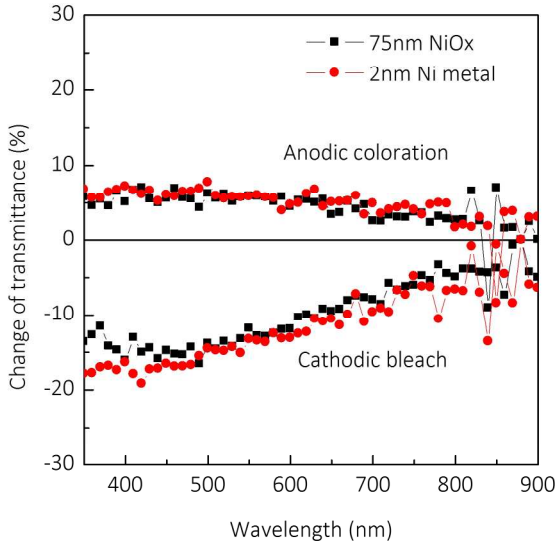

Figure S3. Wavelength-dependent electrochromic properties of NiO_x and ultrathin Ni metal coated FTO glass substrates under anodic operation (1.6 V vs. RHE) and under cathodic (bleach) conditions (0.7 V. vs. RHE) in 1.0 M KOH, respectively.

Supplementary Table:

Table S1. Comparative performances of Si photoanodes for water oxidation

Year/Month	Photoanode	η(%)/condition*	Stability	Ref
2011/06	n-Si|SiO_x|TiO_2|Ir	0.37 / 1 M NaOH (aq)	8 h	[7]
2011/06	npp^+-Si|ITO|Co-Pi	0.04 / 0.1 M K-Pi(aq)	12 h	[8]
2011/11	n-Si|Fe_2O_3	0.04 / 1 M NaOH(aq)	1 h	[9]
2012/04	n-Si|SiO_x|NiO_x	0.006 / 0.25 M PBS Na_2SO_4(aq)	30 m	[10]
2013/02	n-Si|MnO	0.23 / 1 M KOH(aq)	30 m	[11]
2014/01	np^+-Si|ITO:Au|NiO_x	0.07 / 52 mW cm^{-2}, 1 M NaOH(aq)	2.5 h	[12]
2014/01	n-Si|SiO_x|Ni	0.14 / 200 mW cm^{-2}, 1 M KOH (aq)	24 h	[13]
2014/04	np+-Si|SiO_x|CoO_x	0.75 / 1 M NaOH (aq)	24 h	[1]
2014/05	np^+-Si|IrO_x	- / 38.6 mW cm^{-2} λ > 635 nm, 1 M H_2SO_4(aq)	18 h	[14]
2014/05	np^+-Si|TiO_2|Ni islands	0.32 / 125 mW cm^{-2}, 1 M KOH (aq)	100 h	[15]
2014/09	np^+-Si|Ni|NiO_x	- / 38.6 mW cm^{-2} λ > 635 nm, 1 M KOH (aq)	300 h	[16]
2014/12	np^+-Si|NiO_x	2.1 / 1 M KOH (aq)	1200 h	This work

* η (%) is the solar-to-O_2(g) figure-of-merit defined by $(E\text{-}E^{O'}{}_{H2O/O2})_m * J_m/P$, where the product $(E\text{-}E^{O'}{}_{H2O/O2})_m$ and J_m defines the maximum power point relative to the Nernst potential for water oxidation, data point were extracted from the cited original work. Light intensities are 100 mW cm^{-2}, unless specified. "-" indicates that the figure-of-merit cannot be calculated due to the different light source used.

References

1 Yang, J. *et al.* Efficient and Sustained Photoelectrochemical Water Oxidation by Cobalt Oxide/Silicon Photoanodes with Nanotextured Interfaces. *J. Am. Chem. Soc.* **136**, 6191-6194, doi:10.1021/ja501513t (2014).

2 McLean, D. & Feldman, B. Method for etching. United States patent (2006).

3 Shaner, M. R., Fountaine, K. T. & Lewerenz, H. J. Current-voltage characteristics of coupled photodiode-electrocatalyst devices. *Applied Physics Letters* **103**, doi:10.1063/1.4822179 (2013).

4 Mills, T. J., Lin, F. & Boettcher, S. W. *Physical Review Letters* **112**, 148304 (2014).

5 Kibsgaard, J., Jaramillo, T. F. & Besenbacher, F. Building an appropriate active-site motif into a hydrogen-evolution catalyst with thiomolybdate [Mo3S13]2– clusters. *Nat. Chem.* **6**, 248-253, doi:10.1038/nchem.1853

http://www.nature.com/nchem/journal/v6/n3/abs/nchem.1853.html#supplementary-information (2014).

6 Benck, J. D., Chen, Z., Kuritzky, L. Y., Forman, A. J. & Jaramillo, T. F. Amorphous Molybdenum Sulfide Catalysts for Electrochemical Hydrogen Production: Insights into the Origin of their Catalytic Activity. *ACS Catalysis* **2**, 1916-1923, doi:10.1021/cs300451q (2012).

7 Chen, Y. W. *et al.* Atomic layer-deposited tunnel oxide stabilizes silicon photoanodes for water oxidation. *Nat. Mater.* **10**, 539-544, doi:10.1038/nmat3047 (2011).

8 Pijpers, J. J. H., Winkler, M. T., Surendranath, Y., Buonassisi, T. & Nocera, D. G. Light-induced water oxidation at silicon electrodes functionalized with a cobalt oxygen-evolving catalyst. *Proc. Natl. Acad. Sci. USA* **108**, 10056-10061, doi:10.1073/pnas.1106545108 (2011).

9 Jun, K., Lee, Y. S., Buonassisi, T. & Jacobson, J. M. High Photocurrent in Silicon Photoanodes Catalyzed by Iron Oxide Thin Films for Water Oxidation. *Angew. Chem. Int. Ed.* **51**, 423-427, doi:10.1002/anie.201104367 (2012).

10 Sun, K. *et al.* Nickel oxide functionalized silicon for efficient photo-oxidation of water. *Energy Environ. Sci.* **5**, 7872-7877, doi:10.1039/C2EE21708B (2012).

11 Strandwitz, N. C. *et al.* Photoelectrochemical Behavior of n-type Si(100) Electrodes Coated with Thin Films of Manganese Oxide Grown by Atomic Layer Deposition. *J. Phys. Chem. C* **117**, 4931-4936, doi:10.1021/jp311207x (2013).

12 Sun, K. *et al.* Si photoanode protected by a metal modified ITO layer with ultrathin NiOx for solar water oxidation. *Phys. Chem. Chem. Phys.* **16**, 4612-4625, doi:10.1039/C4CP00033A (2014).

13 Kenney, M. J. *et al.* High-Performance Silicon Photoanodes Passivated with Ultrathin Nickel Films for Water Oxidation. *Science* **342**, 836-840, doi:10.1126/science.1241327 (2013).

14 Mei, B. *et al.* Protection of p+-n-Si Photoanodes by Sputter-Deposited Ir/IrOx Thin Films. *J. Phys. Chem. Lett.* **5**, 1948-1952, doi:10.1021/jz500865g (2014).

15 Hu, S. *et al.* Amorphous TiO2 coatings stabilize Si, GaAs, and GaP photoanodes for efficient water oxidation. *Science* **344**, 1005-1009, doi:10.1126/science.1251428 (2014).

16 Mei, B. *et al.* Iron-Treated NiO as a Highly Transparent p-Type Protection Layer for Efficient Si-Based Photoanodes. *J. Phys. Chem. Lett.* **5**, 3456-3461, doi:10.1021/jz501872k (2014).